Exaggerated Left Ventricular Dilation and Reduced Collagen Deposition After Myocardial Infarction in Mice Lacking Osteopontin

Nathan A. Trueblood, Zhonglin Xie, Catherine Communal, Flora Sam, Soeun Ngoy, Lucy Liaw,
Alan W. Jenkins, Jing Wang, Douglas B. Sawyer, Oscar H.L. Bing, Carl S. Apstein,
Wilson S. Colucci, Krishna Singh

Abstract—Osteopontin (OPN), an extracellular matrix protein, is expressed in the myocardium with hypertrophy and failure. We tested the hypothesis that OPN plays a role in left ventricular (LV) remodeling after myocardial infarction (MI). Accordingly, OPN expression and LV structural and functional remodeling were determined in wild-type (WT) and OPN knockout (KO) mice 4 weeks after MI. Northern analysis showed increased OPN expression in the infarcted region, peaking 3 days after MI and gradually decreasing over the next 28 days. In the remote LV, OPN expression was biphasic, with peaks at 3 and 28 days. In situ hybridization and immunohistochemical analyses showed increased OPN mRNA and protein primarily in the interstitium. Infarct size, heart weight, and survival were similar in KO and WT mice after MI (P=NS), whereas the lung wet weight/dry weight ratio was increased in the KO mice ($P<0.005$ versus sham-operated mice). Peak LV developed pressure was reduced to a similar degree after MI in the KO and WT mice. The number of terminal deoxynucleotidyl transferase–mediated dUTP nick end-labeling (TUNEL)-positive myocytes was similar in KO and WT mice after MI. In contrast, post-MI LV chamber dilation was approximately twice as great in KO versus WT mice ($P<0.001$). Myocyte length increased after MI in WT mice ($P<0.001$) but not in KO mice. Electron microscopy showed increased collagen content in WT mice after MI but not in KO mice after MI. Type I collagen content was increased ≈3-fold and ≈7-fold in remote and infarcted regions, respectively, of WT hearts after MI but not in KO hearts ($P<0.01$ versus WT hearts). Likewise, Northern analyses showed increased collagen I(α_1) mRNA after MI in remote regions of WT hearts but not in KO hearts. Thus, increased OPN expression plays an important role in regulating post-MI LV remodeling, at least in part, by promoting collagen synthesis and accumulation. (*Circ Res*. 2001;88:1080-1087.)

Key Words: extracellular matrix proteins ∎ osteopontin ∎ collagen ∎ myocyte slippage ∎ myocyte elongation

---

The dynamic synthesis and breakdown of extracellular matrix (ECM) proteins may play an important role in myocardial remodeling.[1,2] Recently, using spontaneously hypertensive and aortic-banded rats, we showed increased expression of osteopontin (OPN), an ECM protein, coincident with the development of heart failure.[3] Although first isolated from mineralized bone matrix, OPN has since been shown to be synthesized by several cell types, including cardiac myocytes, microvascular endothelial cells, and fibroblasts.[4–6] OPN, an adhesive glycophosphoprotein with an arginine-glycine-aspartic acid (RGD) sequence, has been shown to interact with integrins ($\alpha_V\beta_3$, $\alpha_V\beta_1$, and $\alpha_V\beta_5$) and the CD44 receptor in an RGD-dependent manner.[4,7] OPN appears capable of mediating diverse biological functions, including cell adhesion, chemotaxis, and signaling.[4,8]

OPN has also been shown to interact with fibronectin and collagen, suggesting its possible role in matrix organization and/or stability.[9–11] Recently, using a mammary cell line, we observed that suppression of OPN synthesis leads to increased activity of matrix metalloproteinase (MMP)-2.[12] In fact, there is increased expression of OPN in several tissues in response to injury, suggesting a role in wound healing. Using a skin incision model, Liaw et al[13] observed disorganization of the matrix and alteration of collagen fibrillogenesis, leading to collagen fibrils with smaller diameters in OPN knockout (KO) mice. Similarly, OPN has been shown to play a critical role in the generation of interstitial fibrosis in the kidney after obstructive nephropathy.[14]

Remodeling after myocardial infarction (MI) is associated with left ventricular (LV) dilation, decreased cardiac function, and increased mortality.[15] Early dilation of the LV is likely due to scar expansion in the infarcted region,[16–18] followed later by progressive remodeling[19] in the noninfarcted (remote) LV, which is possibly due to myocyte elongation and/or side-to-side

---

slippage of myocytes.[20,21] Early after MI, the infarcted region of the LV undergoes myocyte necrosis, apoptosis,[18,22] and ECM reorganization.[23–27] Late remodeling in the remote LV may also involve changes in ECM.[28] Alterations in ECM, in particular, increased collagen accumulation[29,30] and changes in the activity of MMPs and tissue inhibitors of metalloproteinase,[2] have been observed in the remote myocardium after MI. These ECM changes may contribute to LV chamber dilation via myocyte lengthening and/or slippage.[20,21,28] However, the underlying mechanisms responsible for matrix reorganization are not clear.

Because OPN expression is increased in pathophysiological conditions and may play an important role in the ECM organization, we hypothesized that OPN is involved in myocardial remodeling after MI. We tested this hypothesis by assessing myocardial structural and functional remodeling with the use of OPN KO mice.

Materials and Methods

Vertebrate Animals

All experiments were performed in accordance with protocols approved by the Institutional Animal Care and Use Committee. Mice lacking OPN (KO mice) and wild-type mice (WT mice) were of a 129×black Swiss hybrid background.[13] Genotyping was carried out by polymerase chain reaction analysis with the use of primers suggested by Liaw et al.[13] Once genotyped, the KO and WT animals were bred and maintained as separate colonies. Personnel blinded to genotype performed all measurements in the present study.

Myocardial Infarction

MI was performed on age-matched mice as previously described.[19,31] After anesthesia, the left coronary artery was occluded with a 7-0 silk suture. Sham-operated animals underwent the same procedure without ligation of the coronary artery. All the experimental measurements were carried out 1 month after MI, except for the measurement of OPN expression in the myocardium after MI (see time-point details in figure legends).

Langendorff Preparation

LV function was measured from the isolated blood-perfused heart preparation as described.[19,31] The hearts were perfused retrogradely via a 20-gauge cannula at a constant perfusion pressure of 70 mm Hg and were paced at 7 Hz. The perfusate consisted of Krebs-Henseleit buffer containing bovine red blood cells adjusted to a hematocrit of 40%.[31] A small fluid-filled balloon was placed in the LV and connected to a pressure transducer for determination of LV pressures. The balloon was then progressively filled in 5-μL increments to generate LV filling and function curves. The chamber stiffness constant (K_c) was determined by fitting the end-diastolic pressure-volume curves from individual hearts to an exponential function as described[33]: $P = b \cdot \exp(K_c V)$, where V is volume, and P is LV pressure.

Fixation for Morphometry

After Langendorff studies, the intra-LV balloon was filled to a distending pressure of 5 mm Hg, and the hearts were arrested in diastole with KCl (30 mmol/L), followed by perfusion fixation with 10% buffered formalin. Infarct size was determined in a manner similar to that of Pfeffer et al.[15] MI size was calculated as the percentage of circumference occupied by scar tissue.

Myocyte Isolation and Length Measurement

Myocytes were isolated by enzyme digestion, as previously reported.[5] Isolated myocytes were fixed in 2% glutaraldehyde and visualized by light microscopy. Myocyte length was determined from a group of hearts (WT-sham, n=3; WT-MI, n=4; KO-sham, n=3; and KO-MI, n=4) by using Bioquant Image analysis software. Approximately 100 myocytes were measured from each heart.

TUNEL Staining

To detect apoptosis, terminal deoxynucleotidyl transferase–mediated dUTP nick end-labeling (TUNEL) staining followed by Hoechst 33258 staining was carried out in 4-μm-thick sections from the LV apex, mid cavity, and base, as previously described.[19] TUNEL-positive nuclei that appeared within the cardiac myocytes were counted. The total number of nuclei per unit area of the heart was estimated by counting the number of Hoechst-positive nuclei under ultraviolet illumination. The number of apoptotic cardiac myocyte nuclei in 15 fields was averaged, and the data were calculated as the percentage of apoptotic myocyte nuclei/total number of nuclei.

Northern Analysis

LV tissue was dissected into infarcted and noninfarcted zones, and total RNA was isolated from the LV according to the method of Chomczynski and Sacchi.[32] Northern analysis was carried out with the use of OPN[5] or collagen I(α_1) (courtesy of Dr Peter Brecher, Boston University School of Medicine, Boston) cDNA probes. To normalize the loading differences, blots were probed with an 18S oligonucleotide end-labeled by T4 polynucleotide kinase.[5] Differences in mRNA signal intensity were determined by using a PhosphorImager (Bio-Rad).

In Situ Hybridization

In situ hybridization for OPN was performed as previously described.[3] Hearts were perfusion-fixed with 4% paraformaldehyde, and 4-μm-thick sections were hybridized with single-stranded sense or antisense RNA probes transcribed from a linearized full-length OPN cDNA with the use of [α-^{35}S]UTP.

Immunohistochemistry

Sections (4 μm thick) from mice hearts were deparaffinized and stained with rabbit collagen type I (Calbiochem) and monoclonal anti-OPN antibodies, as described previously.[3]

Electron Microscopy

Hearts were perfusion-fixed with glutaraldehyde/paraformaldehyde (2%/1%) in 0.1 mol/L phosphate buffer. The LV was then dissected into infarcted and remote regions. For scanning electron microscopy (SEM), the tissue was dehydrated and frozen in liquid nitrogen, followed by freeze fracture. The fractured samples were dried to critical point with CO_2 and sputtered-coated with gold-palladium (60% gold/40% palladium) to 20 nm (Anatech). Samples were examined with a JOEL-6100 SEM at 5 kV. For transmission electron microscopy (TEM, images not shown), tissue slices were postfixed and embedded in Epon plastic. Sections were stained with 1% uranyl acetate and photographed by use of a Philips TEM operating at 120 kV.

Statistical Analysis

Data are reported as mean±SE. Student *t* tests or 2-way ANOVAs followed by Student-Newman-Keuls post hoc tests were used for establishing significant differences among groups. A value of $P < 0.05$ was considered significant.

An expanded Materials and Methods section can be found in the online data supplement available at http://www.circresaha.org.

Results

Expression of OPN in Myocardium After MI

Faint OPN expression was detected in sham-operated animals, suggesting basal expression of OPN in the mouse heart (Figure 1). At day 3 after MI, abundant expression of OPN was detected in the infarcted region ($P < 0.001$ versus sham operation, Figure 1A). OPN mRNA started to decline from its peak 7 days after MI but remained increased above the sham level 14 and 28 days after MI ($P < 0.01$, Figure 1B). In the remote area, OPN expression was increased at 3 days after MI in all hearts, with a range of 4- to 40-fold ($P = 0.05$ versus
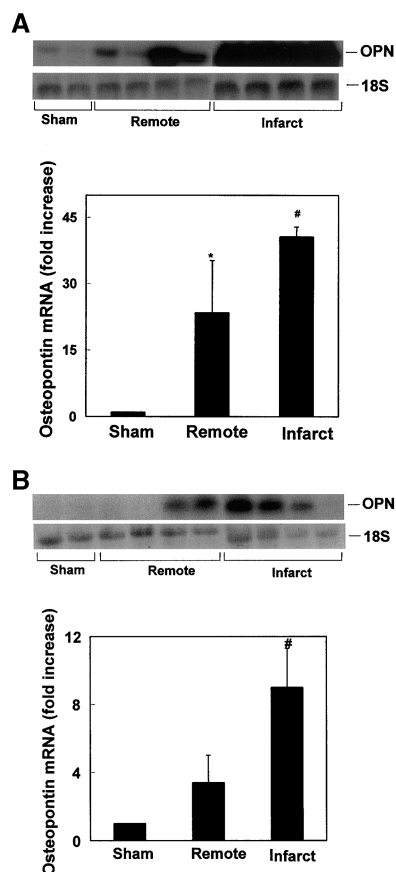
Figure 1. OPN expression after MI assessed by Northern analyses. A, OPN expression 3 days after MI. OPN expression was increased 4- to 40-fold in remote myocardium (*P=0.05 vs sham) and 37- to 46-fold in infarcted tissue (#P<0.001 vs sham). B, OPN expression 28 days after MI. OPN expression was modestly increased in remote myocardium (P=NS) compared with the infarcted tissue (#P<0.01).

Figure 2. A, OPN expression. In situ hybridization with an antisense OPN cRNA probe 7 days after MI. Positive staining for OPN (white grains) was visualized and photographed under dark-field illumination (original magnification ×100). Left, Grains were diffuse and focal in the infarcted region. Right, In the remote LV, grains were diffuse, with focal expression associated with vessels. B, Immunohistochemical staining of LV with use of monoclonal anti-OPN (MPIIIB10) antibodies. Positive staining for OPN protein in the myocardium 1 month after MI was observed mainly in the interstitium (original magnification ×400).

sham operation). Increases in remote LV OPN expression were not detectable 7 and 14 days after MI. At 28 days after MI, 2 of 4 hearts exhibited increased expression.

In situ hybridization using an antisense OPN riboprobe 7 days after MI likewise showed abundant expression of OPN message in the area of infarction (Figure 2). The expression of OPN in the infarcted region was diffuse within the interstitial space, with numerous areas of more focal expression. Diffuse OPN message was als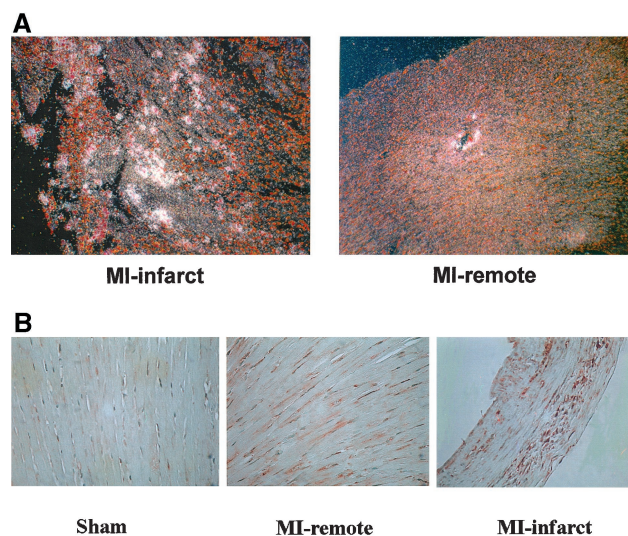o detectable in the remote LV, with more focal message associated with blood vessels, possibly in endothelial and/or smooth muscle cells (Figure 2A). No grains were visible with a sense OPN probe (not shown).

Immunohistochemical analysis demonstrated low levels of immunoreactivity for OPN in the interstitial cells of WT-sham hearts (Figure 2B). In WT-MI hearts, increased staining for OPN was detected in both remote and infarcted regions of the LV. Most of the staining was observed in the interstitium.

Myocardial Infarction, Mortality, and Morphometry

MI size, as a percentage of the LV circumference, was not different between WT and KO-MI groups (P=NS, Figure 3A). The infarcted LV (anterior) free walls were of similar thickness in the 2 MI groups (P=NS, Table). Interestingly, LV mid-papillary circumference, as determined by histology, was increased in the KO-MI group (P<0.05 versus WT-MI

LV Measurements

	Group				
	WT-Sham	KO-Sham	WT-MI	KO-MI	P
HW/BW, mg/g	5.2±0.3	4.8±0.3	6.4±0.3*	6.16±0.2*	<0.05* (WT), <0.01* (KO)
Septal wall, mm	0.93±0.09	0.80±0.06	1.4±0.04*	1.2±0.09*†	<0.001* (WT), <0.01* (KO), 0.06† (WT-KO)
Anterior wall, mm	1.00±0.10	0.90±0.11	0.41±0.04*	0.37±0.07*	<0.001*
LV circumference, mm	12.9±0.45	12.4±0.59	14.7±0.59*	16.5±0.69*†	<0.05* (WT), <0.001* (KO), <0.05† (WT-KO)
K_c, mm Hg	2.75±0.10	3.1±0.42	3.3±0.74	2.2±0.26*	0.09*

Values are mean±SE. HW/BW indicates heart weight/body weight ratio. Septal wall and anterior wall are thicknesses. LV circumference was measured from mid-papillary histological sections.

*Comparisons between sham and MI groups within genotype.

†Comparisons between MI groups.

group, Table). A greater LV circumference in the KO-MI group indicates that although relative infarct size was similar between groups, absolute infarct size was greater in the KO-MI group than in the WT-MI group. The mortality rates in the first 48 hours after MI were 29% and 24% in WT and KO mice, respectively (*P*=NS). There were 2 deaths due to cardiac rupture in each post-MI group, and total mortality 1 month after MI was the same in the 2 groups (53% and 52% in WT and KO mice, respectively, Figure 3B). The lung wet weight/dry weight ratio was increased (10%) in the KO mice but not in WT mice after MI (*P*<0.005 versus KO-sham, Figure 3C).

The heart weight/body weight ratio and septal wall thickness (Table) increased to a similar degree in WT and KO mice after MI (*P*=NS).

LV Pressure-Volume Relationships

LV systolic and diastolic functions were assessed from the LV end-systolic and end-diastolic pressure-volume relationships measured by the isovolumic Langendorff technique. The LV end-diastolic pressure-volume relationship was shifted rightward in WT mice after MI (*P*<0.0001 versus sham-operated mice). The rightward shift was approximately twice as large in KO mice as in WT mice (*P*<0.0001) (Figure 4A). The LV developed pressure-volume relationship was likewise shifted rightward in WT mice after MI (*P*<0.01 versus sham-operated mice), and this shift was greater for the KO mice (*P*<0.05 versus WT mice after MI, Figure 4B). However, the maximal LV developed pressure was depressed to a similar degree in both WT and KO mice after MI (108±8 in WT-MI mice versus 102±10 mm Hg in KO-MI mice, *P*=NS), and the relationship between LV end-diastolic pressure and developed pressure was depressed to a similar degree in WT and KO mice after MI (Figure 4C).

The ratio of LV volume (determined from the Langendorff at an end-diastolic pressure of 10 mm Hg) to heart weight was not increased after MI in WT mice (12.8±1.2 in WT-MI mice versus 11.6±1.9 in WT-sham mice, *P*=NS), suggesting that there had been compensatory hypertrophy. In contrast, the LV volume/heart weight ratio was increased in KO mice after MI (19.2±2.5 in KO-MI mice versus 12.0±1.9 in KO-sham mice, *P*<0.05; *P*<0.05 for KO-MI mice versus WT-MI mice; Figure 5A). The chamber stiffness constant, K_c,[33] decreased after MI in KO mice but not in WT mice, suggesting increased LV diastolic compliance in KO versus WT mice after MI (*P*=0.09, Table).

Myocyte Length

Isolated myocyte length was increased 33% in WT hearts after MI (*P*<0.001 versus sham-operated hearts) (Figure 5B). In KO hearts, myocyte length increased only 9% after MI (*P*=NS versus sham-operated hearts; *P*<0.001 versus WT-MI hearts).

Apoptosis

The number of apoptotic myocytes (calculated as the percentage of apoptotic myocyte nuclei/total number of nuclei) was not different in the myocardium of WT and KO mice 1 month after MI (0.17±0.03 for KO mice, 0.24±0.06 for WT-MI mice; *P*=NS).
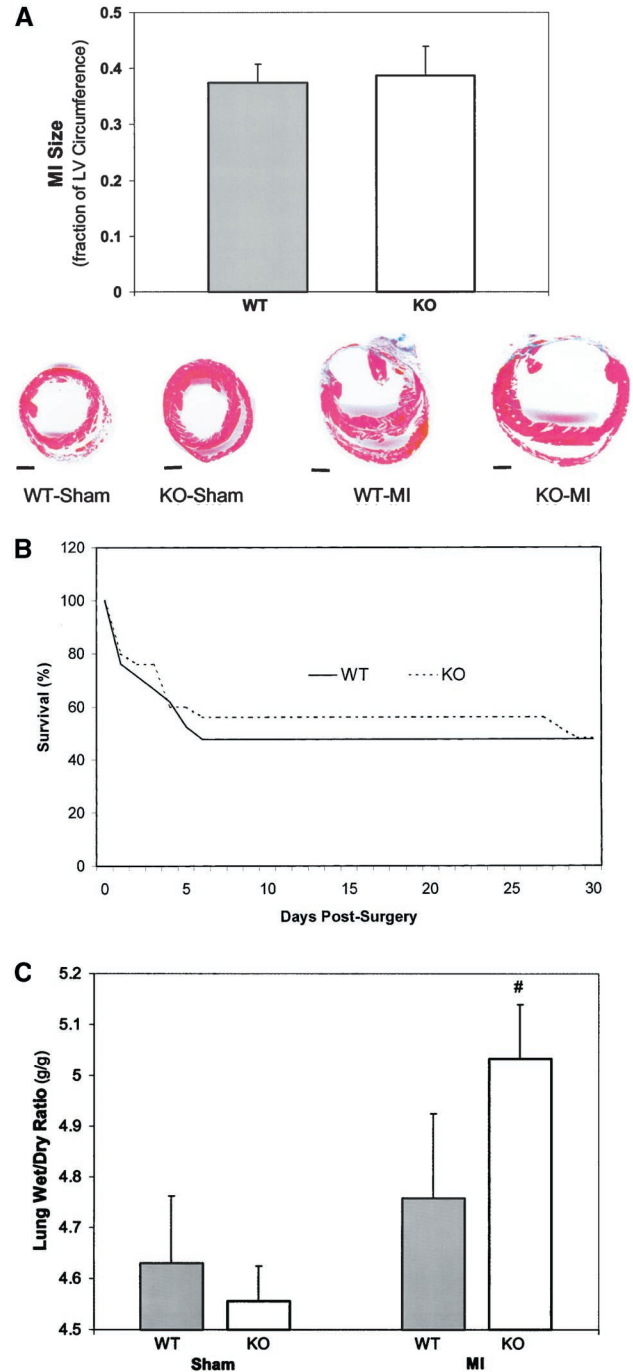

Figure 3. A, Infarct size (top) was calculated as a percentage of LV circumference from Masson's trichrome–stained sections (bottom, bar=1 mm). B, Kaplan-Meier analysis of survival after MI. C, Measurement of pulmonary fluid accumulation as a ratio of wet to dry lung weights. Data are mean±SE. #*P*<0.005 between KO-sham and KO-MI (10% increase).

Changes in Collagen Content

To evaluate the quality of collagen organization in the remote LV, SEM and TEM were performed. Increases in total fibrillar collagen and an increase in the size and frequency of large collagen fibers (struts) were observed in WT-MI mice (compared with WT-sham mice) as analyzed by SEM (Figure 6). Furthermore, total fibrillar collagen appeared reduced in
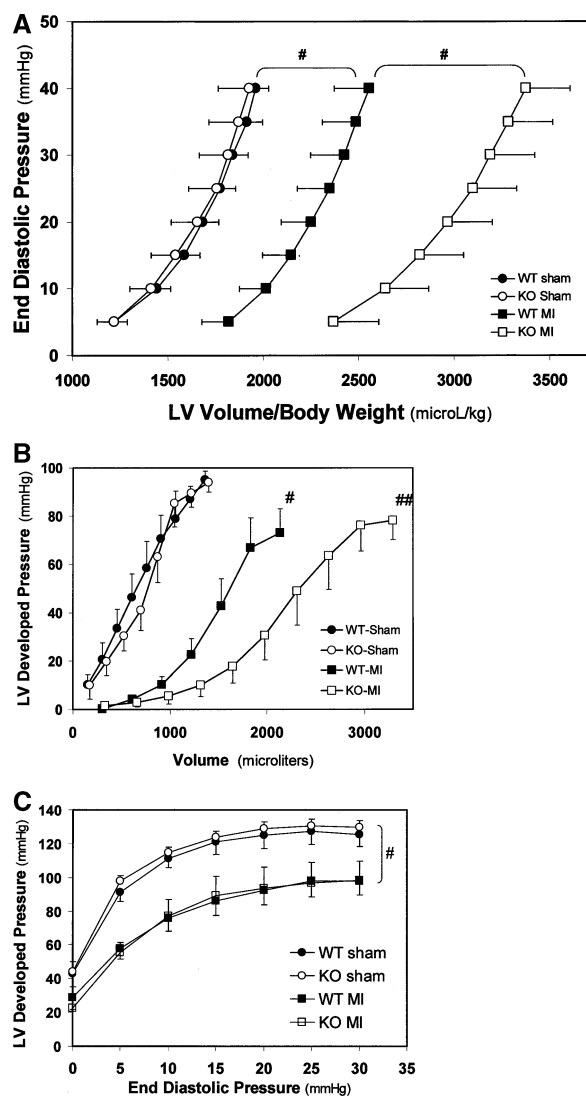
Figure 4. A, Analysis of LV end-diastolic pressure-volume relationships. After MI, WT hearts were significantly dilated compared with WT-sham hearts. KO-MI hearts were significantly dilated compared with WT-MI hearts. #$P<0.0001$. B, Analysis of LV developed pressure versus volume. After MI, hearts were operated at significantly higher volumes to obtain the same LV developed pressure. #$P<0.01$ for WT-MI vs WT-sham; ##$P<0.001$ for KO-MI vs KO-sham; ##$P<0.05$ KO-MI vs WT-MI. C, Analysis of systolic function in the isolated blood-perfused heart. After MI, both KO and WT groups demonstrated significant reductions in LV pressure development (≈30 mm Hg at given end-diastolic pressures). #$P<0.0001$ for WT-MI and KO-MI vs WT-sham and KO-sham.

hearts from KO-MI mice compared with hearts from WT-MI mice. Specifically, there was a marked decrease in thin collagen filaments (weave) between cells, as well as a lack of the larger collagen fibers seen in the WT-MI mice. Similarly, KO-sham mice also appeared to have fewer single collagen filaments between cells compared with WT-sham mice. TEM also exhibited reduced collagen content in KO-MI mice (data not shown).

Immunohistochemical staining of 1-month post-MI heart sections for collagen I demonstrated increases in collagen I content in WT-MI hearts but not in KO-MI hearts (Figure 7A).
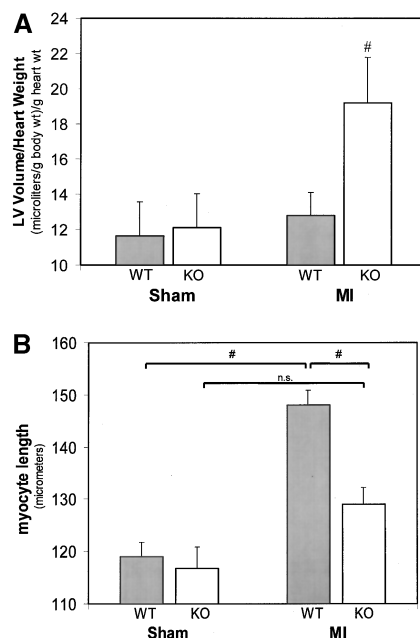

Figure 5. A, Relationship between LV dilation and hypertrophy. LV chamber volume was determined by balloon-in-LV technique and is normalized to body weight. LV dilation in KO-MI hearts was not matched by hypertrophy. #$P<0.05$ vs KO-sham and WT-MI. B, Analysis of myocyte length 1 month after MI. WT-MI myocytes were longer than both WT-sham and KO-MI myocytes. #$P<0.001$.

Quantitative image analysis indicated an ≈3-fold increase in collagen I protein in the remote ($P<0.001$ versus WT-sham mice) and ≈7 fold increase in the infarcted myocardium ($P<0.01$) of WT-MI mice (Figure 7B). KO-MI mice showed no increases in collagen I content ($P<0.01$, WT-MI mice versus KO-MI mice). Likewise, Northern analysis of total RNA isolated from remote LV with the use of a collagen I(α_1) probe demonstrated no significant increase in collagen I mRNA
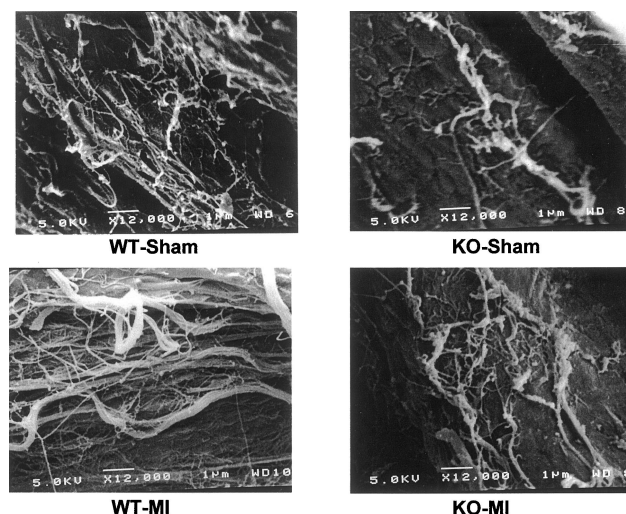

Figure 6. SEM analysis. WT-sham heart tissue showed normal collagen content and fiber size (top left), whereas WT-MI hearts showed increased thin collagen filaments and numerous larger collagen fibers (bottom left). The fibrillar collagen weave appeared reduced or disrupted in the KO group (top right and bottom right).
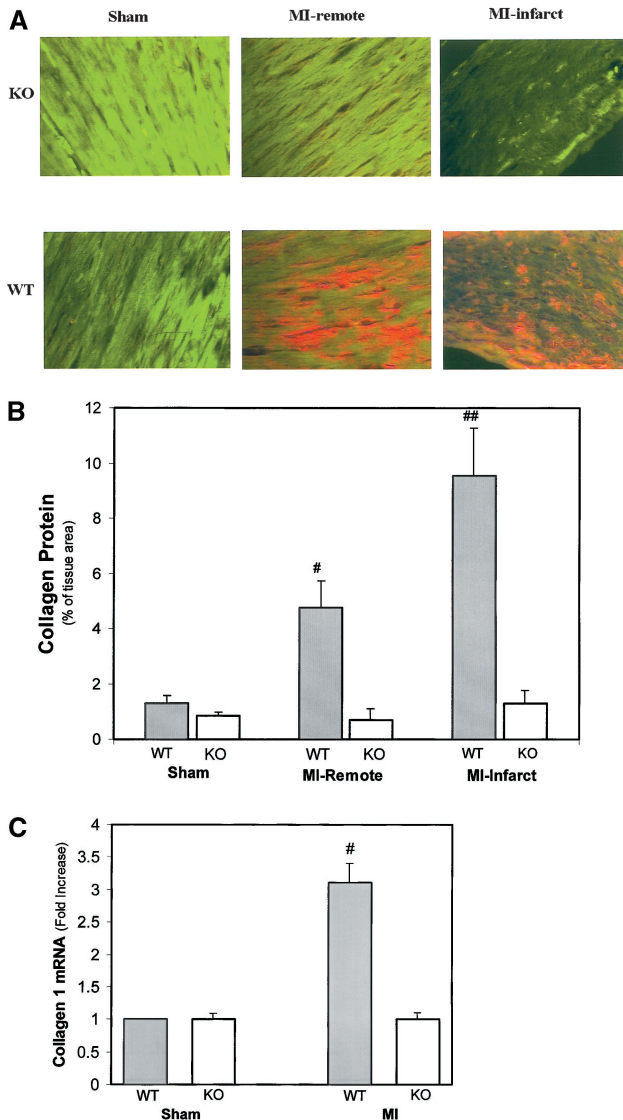
Figure 7. Measurement of collagen I protein and mRNA. A, Immunohistochemical localization of collagen I protein. Collagen I protein was increased in the remote and infarct regions of WT hearts 1 month after MI (original magnification ×400). B, Quantitative image analyses revealed 3- and 7-fold increase in collagen I protein in remote and infarcted regions of WT-MI hearts, respectively. #$P<0.001$ vs WT-sham, ##$P<0.01$ vs all other groups. There was no increase in collagen after MI in KO hearts ($P=$NS). C, Expression of collagen $I(\alpha_1)$ mRNA in the remote LV 1 month after MI assessed by Northern analysis. Collagen $I(\alpha_1)$ mRNA was increased ≈3-fold in the remote LV of WT-MI hearts compared with WT-sham hearts (#$P<0.001$ vs WT-sham). No increase was observed in the remote LV of KO-MI hearts.

expression in KO-MI hearts. However, collagen $I(\alpha_1)$ mRNA was increased 3-fold in the remote LV of WT-MI hearts 1 month after MI (Figure 7C).

Discussion

The major findings of the present study are (1) that OPN expression is increased in the myocardium after MI, (2) that mice lacking OPN have greater LV chamber dilation after MI (compared with WT mice) that is due to increased expansion of both the infarcted and remote myocardium, and (3) that the

lack of OPN is associated with decreased collagen accumulation after MI, which is (at least in part) due to decreased transcription in both the infarcted and remote regions.

Interstitial Expression of OPN After MI

We and others have observed increased myocardial expression of OPN with hypertrophy[3,34] and, particularly, with the transition from hypertrophy to failure.[3] In the present study, we found increased OPN expression in both the infarct and in the myocardium remote from the ischemic injury. In the infarct, OPN expression increased markedly, peaking 3 days after MI, and gradually decreased over the next 28 days. This time course is consistent with an injury response and is similar to that reported by Murry et al[35] after observing thermal injury to the heart. OPN has also been shown to increase in response to injury in other tissues, including lung, skeletal muscle, and skin.[13,35,36]

In contrast to the infarcted area, OPN expression demonstrated a different temporal pattern in remote myocardium. There was a transient increase in OPN mRNA at 3 days. OPN expression returned to sham levels at 7 and 14 days but again increased modestly at 28 days after MI. The expression of OPN in remote myocardium is not likely to reflect an injury response because it was not subjected to a direct injury. Furthermore, the temporal pattern of OPN expression (ie, with a late increase) in remote myocardium would not be consistent with an injury response. Although the stimulus for OPN expression in remote myocardium remains to be determined, both angiotensin[6] and inflammatory cytokines[5] can stimulate OPN expression in cardiac cells in vitro and are known to be increased in remote myocardium after MI.[37–39] In this regard, it is noteworthy that we observed a similar biphasic temporal pattern for the expression of NO synthase 2, which is induced by inflammatory cytokines,[40] in remote myocardium after MI in the mouse.[41]

In situ hybridization revealed that increased expression of OPN in the infarct region was localized primarily to nonmuscle cells and, possibly, infiltrating cells. In the remote region, increased OPN expression was detected primarily in the perivascular space. Increased staining for OPN protein was observed in both the infarct and remote LV of WT-MI hearts. Similar to the in situ hybridization, most of the staining was observed in the interstitial space. This localization is consistent with our prior findings in spontaneously hypertensive myocardium,[3] where the major localization was in nonmyocytes in the interstitium and perivascular space. Likewise, Murry et al[35] and Williams et al[36] found increased OPN expression in the interstitium in rats with thermal injury and in cardiomyopathic hamsters, respectively.

Increased Chamber Dilation After MI in OPN KO Mice

LV chamber volume, as reflected by the Langendorff LV end-diastolic pressure-volume relationship, was significantly increased in WT mice after MI (versus sham). Interestingly, because both heart weight and chamber volume increased to a similar degree in WT-MI animals, the LV volume/heart weight ratio (dilation/hypertrophy index) was not increased in these post-MI animals (versus WT sham-operated animals). However, the chamber volume increase in OPN KO mice was twice as much as in WT-MI mice. Because heart weight

increased to a similar degree in WT and KO mice after MI, the LV volume/heart weight ratio increased in KO versus WT mice after MI. Therefore, these data indicate that (1) the degree of LV dilation in WT mice may have been effectively compensated for by LV hypertrophy, (2) there was a mismatch between chamber dilation and overall myocardial hypertrophy in KO mice after MI, and (3) this mismatch was due to excessive dilation rather than impaired hypertrophy.

LV chamber enlargement after MI is due to (1) infarct expansion, which occurs in the first several days after MI, and (2) dilation of the remote (ie, noninfarcted) myocardium, a progressive process that occurs over weeks to months. Infarct size, measured morphometrically as a fraction of the total LV circumference, was the same in OPN KO and WT mice after MI, suggesting that the increase in chamber volume was due to dilation of both the infarcted and remote regions.

An important aspect of early infarct healing is the deposition of collagen, which stabilizes the damaged myocardium.[23] In the WT mice, there was an ≈7-fold increase in type I collagen in the infarcted region. In striking contrast, this increase in type I collagen was completely absent in the infarcts of the OPN KO mice. The impaired collagen response in OPN KO mice after MI was associated with a lack of increase in collagen I(α_1) mRNA, suggesting that this lack of collagen accumulation after MI is, at least in part, due to decreased expression of collagen I. These data support the thesis that excessive infarct expansion in OPN KO mice was due to impairment of the reparative process. The increase in LV compliance, likewise, may reflect decreased collagen accumulation. In this regard, it is perhaps surprising that cardiac rupture was not more common in KO mice after MI.

After healing of the infarct scar, there is often progressive LV dilation due to remodeling of the remote region.[19] This process may be due to a number of mechanisms, including the loss of myocytes as a result of apoptosis,[18,19,22] myocyte lengthening,[21] and/or side-to-side slippage of myocytes.[20] After MI, there was an ≈3-fold increase in type I collagen in the remote region of WT hearts. These findings suggest that there is increased collagen accumulation in remote myocardium during post-MI remodeling.[29] The marked decrease in collagen accumulation in the KO mice suggests that OPN plays an important role in the regulation of post-MI collagen turnover during remodeling.

There is relatively little increase in myocyte apoptosis in remote myocardium at 1 month after MI,[19] and there was no difference in the frequency of apoptotic myocytes between OPN KO and WT mice. Myocyte length increased by ≈33% in the remote myocardium of the WT mice after MI. This degree of myocyte lengthening adequately explains the degree of chamber dilation in WT mice, suggesting that myocyte lengthening may be one of the primary mechanisms of dilation in 1-month post-MI mice. In striking contrast, there was no myocyte lengthening in the OPN KO mice after MI. Thus, it is unlikely that myocyte apoptosis or lengthening contributed to excessive chamber dilation after MI in OPN KO mice. Therefore, the present data suggest that the major mechanism responsible for increased chamber dilation after MI in the OPN KO mice is a decrease in interstitial collagen deposition leading to the side-to-side slippage of myocytes.[20] These data further raise the possibility that the absence of myocyte lengthening in the OPN

KO mice reflects a decrease in cell-to-cell mechanical forces that is due to decreased collagen.

Our findings are consistent with the evidence that OPN plays an important role in regulating the synthesis and/or turnover of ECM proteins, including collagen.[13,14] In the models of skin incision/wound healing and in obstructive uropathy, disorganization of collagen and decreases in collagen I content were observed in mice lacking OPN.[13,14] OPN can bind directly to collagen I and interacts with collagen II, III, IV, V, and fibronectin.[9–11,42] Furthermore, OPN can affect the expression and activity of matrix metalloproteinases.[12,43] Accordingly, it should be emphasized that our data for collagen I expression were obtained from 1-month post-MI hearts. A thorough time-course analysis of different isoforms of collagen and/or MMPs will be necessary to obtain further insight into the regulation of collagen content by OPN.

After MI in the mouse, LV chamber dilation is associated with a progressive decrease in LV systolic function, as reflected by maximal LV developed pressure, and a progressive increase in the frequency of apoptosis in remote myocardium.[19] In the present study, maximal isovolumic LV developed pressure (ie, maximal LV force generation) was depressed to a similar degree after MI in WT and KO mice, and there was no difference in the frequency of apoptotic myocytes in remote myocardium from WT and KO mice. Taken together, these observations suggest that OPN does not play a direct role in systolic dysfunction or apoptosis of remote region myocytes during post-MI remodeling.

Implications

These data indicate that increased OPN expression after MI protects against LV dilation by promoting collagen synthesis in the infarcted and remote myocardium and, thus, plays an important role in the regulation of post-MI remodeling. These findings have additional, broader implications with regard to the role of collagen in myocardial remodeling. Interstitial fibrosis is a common feature in many forms of cardiomyopathy, and beneficial therapeutic strategies, including ACE inhibition and β-adrenergic receptor blockade, are associated with a net decrease in interstitial fibrosis.[44,45] Therefore, it might be assumed that increased collagen deposition is detrimental. However, these observations in the OPN KO mouse suggest that the relationship between collagen accumulation and increased chamber dilation may not be that simple. An "appropriate" increase in collagen deposition may be an important compensatory response with regard to both infarct repair and the stabilization of myocytes in the remote myocardium.

References

1. Sun Y, Weber KT. Infarct scar: a dynamic tissue. *Cardiovasc Res*. 2000; 46:250–256.
2. Peterson JT, Li H, Dillon L, Bryant JW. Evolution of matrix metalloprotease and tissue inhibitor expression during heart failure progression in the infarcted rat. *Cardiovasc Res*. 2000;46:307–315.
3. Singh K, Sirokman G, Communal C, Robinson KG, Conrad CH, Brooks WW, Bing OH, Colucci WS. Myocardial osteopontin expression coincides with the development of heart failure. *Hypertension*. 1999;33:663–670.
4. Giachelli CM, Schwartz SM, Liaw L. Molecular and cellular biology of osteopontin: potential role in cardiovascular disease. *Trends Cardiovasc Med*. 1995;5:88–95.
5. Singh K, Balligand JL, Fischer TA, Smith TW, Kelly RA. Glucocorticoids increase osteopontin expression in cardiac myocytes and microvascular endothelial cells: role in regulation of inducible nitric oxide synthase. *J Biol Chem*. 1995;270:28471–28478.
6. Ashizawa N, Graf K, Do YS, Nunohiro T, Giachelli CM, Meehan WP, Tuan TL, Hsueh WA. Osteopontin is produced by rat cardiac fibroblasts and mediates A(II)-induced DNA synthesis and collagen gel contraction. *J Clin Invest*. 1996;98:2218–2227.
7. Uede T, Katagiri Y, Iizuka J, Murakami M. Osteopontin, a coordinator of host defense system: a cytokine or an extracellular adhesive protein? *Microbiol Immunol*. 1997;41:641–648.
8. Denhardt DT, Guo X. Osteopontin: a protein with diverse functions. *FASEB J*. 1993;7:1475–1482.
9. Kaartinen MT, Pirhonen A, Linnala-Kankkunen A, Maenpaa PH. Cross-linking of osteopontin by tissue transglutaminase increases its collagen binding properties. *J Biol Chem*. 1999;274:1729–1735.
10. Beninati S, Senger DR, Cordella-Miele E, Mukherjee AB, Chackalaparampil I, Shanmugam V, Singh K, Mukherjee BB. Osteopontin: its transglutaminase-catalyzed posttranslational modifications and cross-linking to fibronectin. *J Biochem (Tokyo)*. 1994;115:675–682.
11. Mukherjee BB, Nemir M, Beninati S, Cordella-Miele E, Singh K, Chackalaparampil I, Shanmugam V, DeVouge MW, Mukherjee AB. Interaction of osteopontin with fibronectin and other extracellular matrix molecules. *Ann N Y Acad Sci*. 1995;760:201–212.
12. Nemir M, Bhattacharyya D, Li X, Singh K, Mukherjee AB, Mukherjee BB. Targeted inhibition of osteopontin expression in the mammary gland causes abnormal morphogenesis and lactation deficiency. *J Biol Chem*. 2000;275:969–976.
13. Liaw L, Birk DE, Ballas CB, Whitsitt JS, Davidson JM, Hogan BL. Altered wound healing in mice lacking a functional osteopontin gene (spp1). *J Clin Invest*. 1998;101:1468–1478.
14. Ophascharoensuk V, Giachelli CM, Gordon K, Hughes J, Pichler R, Brown P, Liaw L, Schmidt R, Shankland SJ, Alpers CE, Couser WG, Johnson RJ. Obstructive uropathy in the mouse: role of osteopontin in interstitial fibrosis and apoptosis. *Kidney Int*. 1999;56:571–580.
15. Pfeffer MA, Pfeffer JM, Fishbein MC, Fletcher PJ, Spadaro J, Kloner RA, Braunwald E. Myocardial infarct size and ventricular function in rats. *Circ Res*. 1979;44:503–512.
16. Weisman HF, Bush DE, Mannisi JA, Weisfeldt ML, Healy B. Cellular mechanisms of myocardial infarct expansion. *Circulation*. 1988;78:186–201.
17. Mannisi JA, Weisman HF, Bush DE, Dudeck P, Healy B. Steroid administration after myocardial infarction promotes early infarct expansion: a study in the rat. *J Clin Invest*. 1987;79:1431–1439.
18. Anversa P, Cheng W, Liu Y, Leri A, Redaelli G, Kajstura J. Apoptosis and myocardial infarction. *Basic Res Cardiol*. 1998;93(suppl 3):8–12.
19. Sam F, Sawyer DB, Chang DL, Eberli FR, Ngoy S, Jain M, Amin J, Apstein CS, Colucci WS. Progressive left ventricular remodeling and apoptosis late after myocardial infarction in mouse heart. *Am J Physiol*. 2000;279: H422–H428.
20. Olivetti G, Capasso JM, Sonnenblick EH, Anversa P. Side-to-side slippage of myocytes participates in ventricular wall remodeling acutely after myocardial infarction in rats. *Circ Res*. 1990;67:23–34.
21. Gerdes AM, Capasso JM. Structural remodeling and mechanical dysfunction of cardiac myocytes in heart failure. *J Mol Cell Cardiol*. 1995;27:849–856.
22. Bialik S, Geenen DL, Sasson IE, Cheng R, Horner JW, Evans SM, Lord EM, Koch CJ, Kitsis RN. Myocyte apoptosis during acute myocardial infarction in the mouse localizes to hypoxic regions but occurs independently of p53. *J Clin Invest*. 1997;100:1363–1372.
23. Jugdutt BI, Musat-Marcu S. Opposite effects of amlodipine and enalapril on infarct collagen and remodelling during healing after reperfused myocardial infarction. *Can J Cardiol*. 2000;16:617–625.
24. Cannon RO III, Butany JW, McManus BM, Speir E, Kravitz AB, Bolli R, Ferrans VJ. Early degradation of collagen after acute myocardial infarction in the rat. *Am J Cardiol*. 1983;52:390–395.
25. Whittaker P, Boughner DR, Kloner RA. Role of collagen in acute myocardial infarct expansion. *Circulation*. 1991;84:2123–2134.
26. Carlyle WC, Jacobson AW, Judd DL, Tian B, Chu C, Hauer KM, Hartman MM, McDonald KM. Delayed reperfusion alters matrix metalloproteinase activity and fibronectin mRNA expression in the infarct zone of the ligated rat heart. *J Mol Cell Cardiol*. 1997;29:2451–2463.
27. Inoue K, Kusachi S, Niiya K, Kajikawa Y, Tsuji T. Sequential changes in the distribution of type I and III collagens in the infarct zone: immunohisto-chemical study of experimental myocardial infarction in the rat. *Coron Artery Dis*. 1995;6:153–158.
28. Weber KT, Sun Y, Tyagi SC, Cleutjens JP. Collagen network of the myocardium: function, structural remodeling and regulatory mechanisms. *J Mol Cell Cardiol*. 1994;26:279–292.
29. Lutgens E, Daemen MJ, de Muinck ED, Debets J, Leenders P, Smits JF. Chronic myocardial infarction in the mouse: cardiac structural and functional changes. *Cardiovasc Res*. 1999;41:586–593.
30. Van Kerckhoven R, Kalkman EA, Saxena PR, Schoemaker RG. Altered cardiac collagen and associated changes in diastolic function of infarcted rat hearts. *Cardiovasc Res*. 2000;46:316–323.
31. Eberli FR, Sam F, Ngoy S, Apstein CS, Colucci WS. Left-ventricular structural and functional remodeling in the mouse after myocardial infarction: assessment with the isovolumetrically-contracting Langendorff heart. *J Mol Cell Cardiol*. 1998;30:1443–1447.
32. Chomczynski P, Sacchi N. Single-step method of RNA isolation by acid guanidinium thiocyanate-phenol-chloroform extraction. *Anal Biochem*. 1987; 162:156–159.
33. Pfeffer JM, Pfeffer MA, Fletcher PJ, Braunwald E. Progressive ventricular remodeling in rat with myocardial infarction. *Am J Physiol*. 1991;260: H1406–H1414.
34. Graf K, Do YS, Ashizawa N, Meehan WP, Giachelli CM, Marboe CC, Fleck E, Hsueh WA. Myocardial osteopontin expression is associated with left ventricular hypertrophy. *Circulation*. 1997;96:3063–3071.
35. Murry CE, Giachelli CM, Schwartz SM, Vracko R. Macrophages express osteopontin during repair of myocardial necrosis. *Am J Pathol*. 1994;145: 1450–1462.
36. Williams EB, Halpert I, Wickline S, Davison G, Parks WC, Rottman JN. Osteopontin expression is increased in the heritable cardiomyopathy of Syrian hamsters. *Circulation*. 1995;92:705–709.
37. Ono K, Matsumori A, Shioi T, Furukawa Y, Sasayama S. Cytokine gene expression after myocardial infarction in rat hearts: possible implication in left ventricular remodeling. *Circulation*. 1998;98:149–156.
38. Sun Y, Zhang JQ, Zhang J, Ramires FJ. Angiotensin II, transforming growth factor-β_1 and repair in the infarcted heart. *J Mol Cell Cardiol*. 1998;30: 1559–1569.
39. Yue P, Massie BM, Simpson PC, Long CS. Cytokine expression increases in nonmyocytes from rats with postinfarction heart failure. *Am J Physiol*. 1998; 275:H250–H258.
40. Kelly RA, Balligand JL, Smith TW. Nitric oxide and cardiac function. *Circ Res*. 1996;79:363–380.
41. Sam F, Sawyer DB, Ngoy S, Chang DL, Brenner DA, Siwik DA, Singh K, Apstein CS, Colucci WS. Lack of NOS2 improves ventricular remodeling late after myocardial infarction. *Circulation*. 1999;100(suppl I):I-250. Abstract.
42. Butler WT. Structural and functional domains of osteopontin. *Ann N Y Acad Sci*. 1995;760:6–11.
43. Bendeck MP, Irvin C, Reidy M, Smith L, Mulholland D, Horton M, Giachelli CM. Smooth muscle cell matrix metalloproteinase production is stimulated via $\alpha_{V\beta3}$ integrin. *Arterioscler Thromb Vasc Biol*. 2000;20:1467–1472.
44. Jugdutt BI, Lucas A, Khan MI. Effect of angiotensin-converting enzyme inhibition on infarct collagen deposition and remodelling during healing after transmural canine myocardial infarction. *Can J Cardiol*. 1997;13:657–668.
45. Vatner DE, Asai K, Iwase M, Ishikawa Y, Shannon RP, Homcy CJ, Vatner SF. β-adrenergic receptor-G protein-adenylyl cyclase signal transduction in the failing heart. *Am J Cardiol*. 1999;83:80H–85H.